Available online at www.sciencedirect.com
SCIENCE DIRECT®
Computers & Fluids 33 (2004) 771–782
computers & fluids
www.elsevier.com/locate/compfluid

A Dirichlet/Neumann domain decomposition method for incompressible turbulent flows on overlapping subdomains

G. Houzeaux, R. Codina *

International Center for Numerical Methods in Engineering (CIMNE), Edificio C1, Universtitat Politècnica de Catalunya (UPC), Jordi Girona 1-3, 08034 Barcelona, Spain

Received 19 July 2002; received in revised form 6 June 2003; accepted 6 June 2003

Abstract

When one wants to simulate flows with moving bodies and when there is no possible way of prescribing simple boundary conditions in any frame of reference, one possibility is the use of domain decomposition methods. The domain decomposition method we present in this work aims at coupling overlapping subdomains in relative motion using a Dirichlet/Neumann coupling. The method is applied to the solution of incompressible and turbulent flows.

1. Introduction

Classical domain decomposition methods can be divided into overlapping and non-overlapping methods [12]. The Schwarz method [10] consists in solving two Dirichlet problems on overlapping subdomains. The main advantage of Schwarz method is the easy way of dividing the subdomains from a possibly complicated geometry. The main drawback is that the convergence of the iteration-by-subdomain depends on the overlap. Contrary to the Schwarz method, non-overlapping domain decomposition (DD) methods use necessarily two different transmission conditions on the interface, in such a way that both the continuity of the unknown and its first derivatives are achieved on the interface (for the advection–diffusion–reaction equation). The main advantage of

* Corresponding author.
E-mail addresses: houzeaux@cimne.upc.es (G. Houzeaux), ramon.codina@upc.es (R. Codina).
URLs: http://www.rmee.upc.es/homes/houzeaux, http://www.rmee.upc.es/homes/codina.

0045-7930/$ - see front matter
doi:10.1016/j.compfluid.2003.06.010

these methods is that good convergence can be obtained, especially in the case of the Robin/Robin method [11] for which the Robin coefficients can be adjusted to accelerate convergence. However, these methods suffer from the need of coincidence of the subdomain boundaries.

In this work we propose to study a Dirichlet/Neumann (D/N) method allowing overlap between the subdomains. This method exhibits good convergence of the iteration-by-subdomain schemes, and the limit of zero overlap is possible. In addition, it enables an easy division of the computational subdomains as there is no need of coincidence of the subdomain boundaries. In fact, the method introduced here has been successfully used by the authors [8] to devise a Chimera method based on a Dirichlet/Neumann or Dirichlet/Robin (D/R) coupling for solving the incompressible Navier–Stokes equations. In [7], the convergence of the D/R method is proved for the advection–diffusion–reaction equation solved on overlapping subdomains and the numerical performance of the method is studied through numerical examples. In particular, the overlapping versions of the D/N and D/R are compared to their disjoint counterparts as well as to the classical Schwarz method. They show the gain in convergence achieved by overlapping the subdomains. The present paper gives the extension of the D/N method to the solution of turbulent flows on overlapping subdomains.

2. Problem statement and numerical model

2.1. Turbulent incompressible flow equations

We consider turbulent incompressible flows. In order to include turbulence effects into the classical Navier–Stokes equations, we use the Reynolds averaging approach. This method leads to the well-known Reynolds averaged Navier–Stokes (RANS) equations, which involve and extra unknown, the Reynolds stress tensor. This tensor is modeled using the Boussinesq approximation, which at its turn introduces a new unknown, the eddy viscosity ν_t. In this work, this eddy viscosity is computed with a one-equation turbulence model, namely the Spalart–Allmaras (SA) model [13].

The momentum equations are expressed in a non-inertial frame of reference. We denote $\boldsymbol{\omega}$ as the angular velocity of the frame of reference and $\boldsymbol{x}$ the position vector of a fluid point. Let Ω be an open bounded domain of $\mathbb{R}^{n_d}$ ($n_d = 2$ or 3) and $(0, T)$ be the time interval of study. The RANS equations for the mean velocity $\boldsymbol{u}$ and mean pressure p are

$$\mathscr{N}(\boldsymbol{u}, p) = \mathscr{F} \quad \text{in } \Omega \times (0, T),$$

with

$$\mathscr{N} := \begin{bmatrix} \partial_t \boldsymbol{u} + (\boldsymbol{u} \cdot \nabla)\boldsymbol{u} + 2\boldsymbol{\omega} \times \boldsymbol{u} - 2\nabla \cdot [(\nu + \nu_t)\boldsymbol{\varepsilon}(\boldsymbol{u})] + \nabla p \\ \nabla \cdot \boldsymbol{u} \end{bmatrix}, \qquad \mathscr{F} := \begin{bmatrix} \boldsymbol{f} \\ 0 \end{bmatrix},$$

where $\boldsymbol{f} = -\boldsymbol{\omega} \times (\boldsymbol{\omega} \times \boldsymbol{x}) - \mathrm{d}\boldsymbol{\omega}/\mathrm{d}t \times \boldsymbol{x}$ is the vector of body forces, including the non-inertial terms and $\boldsymbol{\varepsilon}(\boldsymbol{u}) = \frac{1}{2}(\nabla \boldsymbol{u} + \nabla \boldsymbol{u}^t)$ is the rate of deformation tensor.

The Navier–Stokes equations must be supplied with initial and boundary conditions. We consider here conditions of Dirichlet, Neumann and mixed types:

$$\begin{aligned} \boldsymbol{u} &= \boldsymbol{u}_g \quad \text{on } \Gamma_{\mathrm{D}} \times (0,T), \\ \boldsymbol{\sigma}\cdot\boldsymbol{n} &= \boldsymbol{t}_n \quad \text{on } \Gamma_{\mathrm{N}} \times (0,T), \\ \boldsymbol{u}\cdot\boldsymbol{n} = 0, \quad \boldsymbol{g}_1\cdot\boldsymbol{\sigma}\cdot\boldsymbol{n} = t_1, \quad \boldsymbol{g}_2\cdot\boldsymbol{\sigma}\cdot\boldsymbol{n} &= t_2 \quad \text{on } \Gamma_{\mathrm{M}} \times (0,T), \\ \boldsymbol{u} &= \boldsymbol{u}_0 \quad \text{on } \Omega \times \{0\}, \end{aligned}$$

where $\Gamma = \Gamma_{\mathrm{N}} \cup \Gamma_{\mathrm{D}} \cup \Gamma_{\mathrm{M}}$, $\boldsymbol{n}$ is the outward unit normal, $\boldsymbol{g}_1$ and $\boldsymbol{g}_2$ are the unit vectors spanning the space tangent to Γ_{M}, $t_1 = \boldsymbol{t}_{\mathrm{t}}\cdot\boldsymbol{g}_1$ and $t_2 = \boldsymbol{t}_{\mathrm{t}}\cdot\boldsymbol{g}_2$ are the components of the tangential traction $\boldsymbol{t}_{\mathrm{t}}$ and $\boldsymbol{\sigma}$ is the stress tensor given by $\boldsymbol{\sigma} = -p\boldsymbol{I} + 2(\nu + \nu_{\mathrm{t}})\boldsymbol{\varepsilon}(\boldsymbol{u})$, $\boldsymbol{I}$ being the n_{d}-dimensional identity. We have chosen as Neumann condition the prescription of the traction $\boldsymbol{\sigma}\cdot\boldsymbol{n}$ because it usually enters naturally the variational form of the problem. The boundary condition of mixed type is imposed on Γ_{M}. For example, in the numerical simulation of turbulent flows, it is common to consider an impermeable wall condition together with the prescription of the tangential component of the traction $\boldsymbol{t}_{\mathrm{t}}$ to emulate the frictional effects of turbulent boundary layers. This will be explained in Section 2.3.

2.2. Turbulence model

The turbulence model chosen to compute the eddy viscosity is the Spalart–Allmaras turbulence model. This model was devised "using empiricism and arguments of dimensional analysis, Galilean invariance, and selective dependence on molecular viscosity" [13]. It consists of a transport equation for the eddy viscosity ν_{t}. For any details on the equation, see the original publication of the authors [13]. We symbolically write the equation as

$$\mathscr{S}(\nu_{\mathrm{t}}) = 0 \quad \text{in } \Omega \times (0,T),$$

with

$$\mathscr{S}(\nu_{\mathrm{t}}) := \partial_{\mathrm{t}}\nu_{\mathrm{t}} + \boldsymbol{u}\cdot\nabla\nu_{\mathrm{t}} - c_{b_1}S\nu_{\mathrm{t}} - \frac{1}{\sigma}\left[\nabla\cdot(\nu_{\mathrm{t}}\nabla\nu_{\mathrm{t}}) + c_{b_2}(\nabla\nu_{\mathrm{t}})^2\right] + c_{w_1}f_w\frac{\nu_{\mathrm{t}}^2}{d^2},$$

where c_{b_1}, c_{b_2}, σ and c_{w_1} are constants, S is the norm of the vorticity, f_w is a function depending on S, ν_{t} and the distance to the wall d. This equation is the high Reynolds number version of the model. Additional corrections enable for example to compute low Reynolds number and transition effects. This equation must be supplied with appropriate initial and boundary conditions.

2.3. Wall function approach

The RANS and turbulence equations are solved using the wall function approach [2] on the wall-type boundaries of the computational domain. In order to avoid solving for the large gradients present in the boundary layer, the wall function approach implemented here consists in assuming that the computational wall is located at a distance Δ sufficiently far from the real wall where the no-slip condition for the velocity holds. Then the wall friction U_* is estimated applying the Log-law of the wall at Δ. For the momentum equations, the boundary condition on the walls is a mixed condition where the normal component of the velocity is zero and where the tangential component of the traction is given by $\boldsymbol{t}_{\mathrm{t}} = -U_*^2\boldsymbol{u}/|\boldsymbol{u}|$. The wall condition for the eddy viscosity is

computed using the classical mixing length hypothesis together with the Van-Driest damping function, i.e. we impose that

$$\nu_t = l_{mix}^2 |\partial u/\partial y|,$$

where the mixing length is given by

$$l_{mix} = \kappa\delta^+[1 - \exp(-\delta^+/26)],$$

with u being the tangential velocity, y the normal axis to the wall and $\delta^+ = \delta U_*/\nu$ the non-dimensional distance to the wall (see for example [14]).

2.4. Numerical strategy

The RANS equations are solved using a Finite Element model based on a stabilized Galerkin method. In fact, it is well-known that the Galerkin formulation can lack stability for three major reasons. The first reason is related to the compatibility of the finite element spaces for the velocity and the pressure which have to satisfy the so-called Ladyzhenskaya–Brezzi–Babuška (LBB) condition. This condition is necessary to obtain a stability estimate for the pressure; without requiring this condition, the pressure would be out of control. The second reason is attributed to the relative importance of the viscous and convective effects. Finally, the third one appears when the Coriolis force becomes important with respect to viscous effects. The stabilized formulation is based on the algebraic variational subgrid scale (SGS) model first introduced in [9]. The variational SGS model uses as a starting argument that the lack of resolution achieved by the mesh is responsible for the numerical instabilities. Therefore, the model calculates in some approximate way the unresolved scales of the flow, i.e. the scales smaller than the mesh size. The method is extensively described in [4]. Finally, the time discretization is carried out using the generalized trapezoidal rule, i.e. a finite difference scheme.

In this work we will consider two types of elements using both equal order interpolation for the velocity and the pressure. The Q1/Q1 element is continuous and bilinear (trilinear in three dimensions) in both velocity and pressure. We will also work with the P1/P1 element, continuous and linear in velocity and pressure. These elements do not satisfy the LBB condition and therefore require the use of stabilization.

A similar numerical model is used to solve the equation for the turbulent viscosity ν_t, which is interpolated like $\boldsymbol{u}$ and p. It is integrated in time using the generalized trapezoidal rule and the algebraic SGS method is employed to stabilize the possible dominance of convective and reactive terms. See [4] for further details.

3. Iteration-by-subdomain method

Let Ω_1 and Ω_2 be two overlapping subdomains, and define Γ_a as the part of $\partial\Omega_2$ lying in Ω_1, and Γ_b as the part of $\partial\Omega_1$ lying in Ω_2, formally given by

$$\Gamma_a := \overline{\partial\Omega_2 \cap \Omega_1}, \qquad \Gamma_b := \overline{\partial\Omega_1 \cap \Omega_2}.$$

Γ_b and Γ_a are the *interfaces* of the domain decomposition method we now present. In the following, subindices refer to the solution obtained on a subdomain.

Box 1. Domain decomposition algorithm

Set $\boldsymbol{u}_1^0 = \boldsymbol{u}^0|_{\Omega_1}$, $\boldsymbol{u}_2^0 = \boldsymbol{u}^0|_{\Omega_2}$
For $n = 1, \ldots, N$ do (time steps)
  Initialize $\boldsymbol{u}_1^{n,0} = \boldsymbol{u}_1^{n-1}$, $\boldsymbol{u}_2^{n,0} = \boldsymbol{u}_2^{n-1}$
  $i = 0$
  While (non-linear iteration not converged) do
    $i \leftarrow i + 1$
    Initialize $\boldsymbol{u}_1^{n,i,0} = \boldsymbol{u}_1^{n,i-1}$, $\boldsymbol{u}_2^{n,i,0} = \boldsymbol{u}_2^{n,i-1}$
    $k = 0$
    While (DD iteration not converged) do
     $k \leftarrow k + 1$

$$
\begin{cases}
\mathscr{N}(\boldsymbol{u}_1^{n,i,k}, p_1^{n,i,k}) = \mathscr{F}, & \\
\mathscr{S}(v_{t_1}^{n,i,k}) = 0 & \text{in } \Omega_1, \\
\text{Boundary conditions} & \text{on } \partial\Omega_1 \cap \partial\Omega, \\
\boldsymbol{u}_1^{n,i,k} = \boldsymbol{u}_2^{n,i,k-1}, & \\
v_{t_1}^{n,i,k} = v_{t_2}^{n,i,k-1} & \text{on } \Gamma_b, \\
\mathscr{N}(\boldsymbol{u}_2^{n,i,k}, p_2^{n,i,k}) = \mathscr{F}, & \\
\mathscr{S}(v_{t_2}^{n,i,k}) = 0 & \text{in } \Omega_2, \\
\text{Boundary conditions} & \text{on } \partial\Omega_2 \cap \partial\Omega, \\
\Phi(\boldsymbol{u}_2^{n,i,k}, p_2^{n,i,k}) = \Phi(\boldsymbol{u}_1^{n,i,k}, p_1^{n,i,k}), & \\
\Psi(v_{t_2}^{n,i,k}) = \Psi(v_{t_1}^{n,i,k}) & \text{on } \Gamma_a.
\end{cases}
$$

  end

The D/N method with overlapping we propose is given in Box 1. There, the functions Φ and Ψ are the traction and the eddy viscosity flux, given respectively by

$$\Phi(\boldsymbol{u}, p) := -p\boldsymbol{n}_2 + 2(\nu + \nu_t)\boldsymbol{\varepsilon}(\boldsymbol{u}) \cdot \boldsymbol{n}_2,$$

$$\Psi(\nu_t) := \frac{1}{\sigma}(\nu_t \nabla \nu_t) \cdot \boldsymbol{n}_2,$$

with $\boldsymbol{n}_2$ being the outward unit normal to Ω_2.

Algorithm of Box 1 is a sequential iteration-by-subdomain method using Dirichlet transmission conditions on Γ_b and Neumann transmission conditions on Γ_a. In addition, we have introduced

two relaxation parameters θ_D and θ_N for the Dirichlet and Neumann conditions, respectively. That is, the Dirichlet conditions on Γ_b are replaced by

$$\boldsymbol{u}_1^{n,i,k} = \theta_D \boldsymbol{u}_2^{n,i,k-1} + (1-\theta_D)\boldsymbol{u}_1^{n,i,k-1},$$

$$v_{t_1}^{n,i,k} = \theta_D v_{t_2}^{n,i,k-1} + (1-\theta_D) v_{t_1}^{n,i,k-1},$$

and the Neumann conditions on Γ_a are replaced by

$$\Phi(\boldsymbol{u}_2^{n,i,k}, p_2^{n,i,k}) = \theta_N \Phi(\boldsymbol{u}_1^{n,i,k}, p_1^{n,i,k}) + (1-\theta_N)\Phi(\boldsymbol{u}_2^{n,i,k-1}, p_2^{n,i,k-1}),$$

$$\Psi(v_{t_2}^{n,i,k}) = \theta_N \Psi(v_{t_1}^{n,i,k}) + (1-\theta_N)\Psi(v_{t_2}^{n,i,k-1}).$$

Let us note that the RANS and turbulence equations are decoupled sequentially as described in [1]. Likewise, the non-linear iteration and DD loops can be coupled.

4. Implementation aspects

We review here some implementation aspects of the Algorithm of Box 1. The points we are going to expose are the following: master/slave algorithm; imposition of the transmission conditions; conservation; element search strategy; treatment of moving subdomains. For any details, see [8].

The iteration-by-subdomain method is implemented within a *master/slave algorithm*. Each subdomain is solved independently using a fluid solver. The coupling between the subdomains is performed by a master code, which is in charge of controlling the iterative process and performing all the necessary operations to leave the slaves unworried. This method is very efficient as almost no modification to the original fluid solver is necessary.

The main task of the master is the update of the transmission conditions. As a first approach, the Dirichlet-type transmission conditions are imposed at the nodes of the interface using the classical Lagrange interpolation functions. In order to avoid any possible loss of information when passing Dirichlet data from one subdomain to another, an interface constraining is introduced: continuity of the transmission conditions are constrained under a scalar *conservation equation*. This approach is explained in [5], where an example of mass conservation is considered. The Neumann-type transmission conditions are imposed as force terms in the momentum and eddy viscosity equations. The force terms are the integrals of the traction and the eddy viscosity flux along the interface, respectively. The strain rates as well as the eddy viscosity gradient are therefore needed at some integration points. All the derivatives involved in these terms are calculated using a least-square smoothing. In order to achieve a good approximation in space, these derivatives need to be calculated with one layer of elements on each side of the interface. This is explained in [6].

The element search task consists in finding the host element of a node or integration point of the interface on the underlying mesh. If the subdomains are moving, this task may be expensive and an efficient algorithm is required. The method we use here is based on a quad(oct)-tree decomposition of the underlying mesh.

Finally, when subdomains are moving, tensorial transformations are necessary to compute variables from one subdomain to another. These variables are: coordinates, velocity, strain rates and eddy viscosity gradient. In order to integrate frames of reference with possibly complicated rotation vectors, we use a second order scheme in time.

5. Numerical examples

5.1. Backward facing step

We solve the turbulent backward facing step using the overlapping D/N method and compare the results with a one-domain solution and with the results of a D/N method applied to disjoint subdomains. The step height is H, the channel height $2H$, the channel entrance is $6H$-long and the total length of the computational domain is $50H$. The inlet velocity profile is uniform such that $\boldsymbol{u} = (U, 0)$. The Reynolds number based on H and U is $Re = 70\,000$.

We decompose the domain vertically into two overlapping subdomains and two disjoint subdomains, for which the interfaces fall inside the recirculation zone. For the overlapping D/N method, the overlap is $0.5H$. Through this example we want to appreciate the effects of the overlap on the convergence of the algorithm, even when the transmission conditions are placed indifferently with respect to the flow direction. The meshes of each subdomain are such that they approximately mimic the mesh used for the one-domain solution. The left-hand side subdomain is meshed with 880 Q1/Q1 elements for the overlapping configuration and with 800 Q1/Q1 elements for the disjoint configuration. The right-hand side subdomain is the same for the overlapping and disjoint methods and comprises 1600 Q1/Q1 elements. The mesh used for the one-domain solution comprises 2000 Q1/Q1 elements. A zoom around the step corner of the composite meshes and one-domain mesh are shown in Fig. 2(top left), (top middle) and (top right). The problem is solved using the wall function approach with $\Delta/H = 4.0\%$, where Δ is the distance of the computational wall to the real wall. The inflow eddy viscosity is $\nu_t/\nu = 100$.

The interface of the left subdomain is of Neumann type while that of the right subdomain is of Dirichlet type. Fig. 1(left) and (right) show the convergence history of the overlapping method obtained for two combinations of the relaxation parameters θ_D and θ_N. Both combinations lead to convergence of the overlapping D/N method. For the sake of comparisons, Table 1 compares the

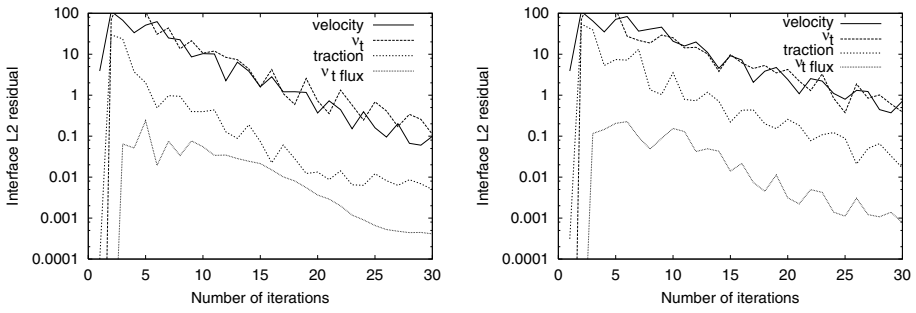

Fig. 1. Backward facing step. Convergence history. (Left) $\theta_D = 1.0$, $\theta_N = 0.3$. (Right) $\theta_D = 1.0$, $\theta_N = 1.0$.

Table 1
Number of iterations to achieve convergence

θ_D	θ_N	Disjoint	Overlapping
0.3	0.3	45	22
0.3	1.0	–	22
1.0	0.3	–	26
1.0	1.0	–	29

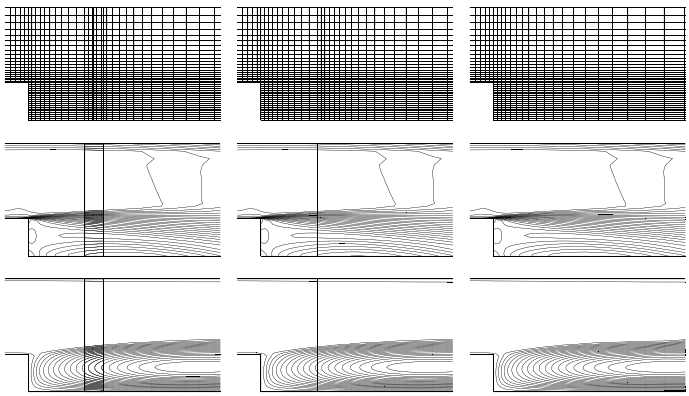

Fig. 2. Backward facing step. From left to right: overlapping D/N, disjoint D/N, one-domain. From top to bottom: mesh, velocity contours, eddy viscosity contours.

number of iterations needed to achieve convergence for different relaxation parameters using the disjoint and overlapping methods. Convergence is achieved when the Euclidean norm of the interface residual of the velocity is below $10^{-1}\%$. We observe the positive effects of the overlapping on the convergence of the method. The minus sign indicates that the method does not converge.

Fig. 2 compares the contours of velocity module and eddy viscosity obtained with the two D/N methods and the one-domain simulation. The profiles are identical and confirm the good convergence of the DD algorithm.

5.2. Centrifugal fan

We propose to solve a two-dimensional section of a domestic centrifugal fan. The geometry as well as the data are based on the CK-40 fan of Soler-i-Palau (a fan manufacturer), shown in Fig. 3(left). The dimensions of the impeller and the casing of the fan are $R_1 = 80$ mm, $R_2 = 40$ mm, $R_3 = 31$ mm, $L_1 = 126$ mm, $L_2 = 88$ mm, $L_3 = 50$ mm, $L_4 = 94$ mm, $L_5 = 106$ mm, $L_6 = 125$ mm.

The mass flow rate is imposed at the inflow, through the specification of the velocity, and zero traction is imposed at the outflow, which corresponds to a zero pressure if the flow is fully developed. The inflow velocity $\boldsymbol{U}$ is imposed normal to the circular inlet of radius R_3, as sketched in Fig. 3(right). The Reynolds number based on the inflow velocity $|\boldsymbol{U}| = 1.97 \times 10^3$ mm/s and the

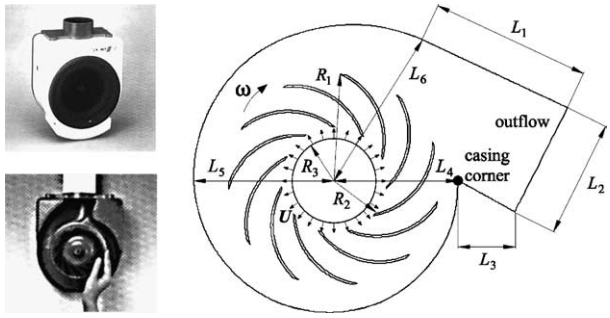

Fig. 3. CK-40 fan. (Left) Pictures of the fan. (Right) Two-dimensional section.

length of the inlet $D = 2\pi R_3 = 201.06$ mm is $Re = 2.65 \times 10^4$, v being the kinematic viscosity of air, $v = 15$ mm^2/s. The angular speed is $|\omega| = 246.09$ rad/s.

Due to the high Reynolds number, the flow is solved using the Spalart–Allmaras turbulence model together with the wall function approach. The inflow turbulence viscosity is $v_t/v = 100$ and the distance from the computational wall to the real wall is set to $\Delta/D = 2.1\%$ for the inner subdomain and to $\Delta/D = 0.6\%$ for the outer subdomain.

The fan is divided into two subdomains, one attached to the impeller and the other attached to the casing. In order to couple the subdomains, we assign the impeller a Neumann transmission condition while the casing interface is of Dirichlet type and we impose an overlap of the subdomains of at least one element layer. The impeller domain is meshed with 12 782 P1/P1 elements and the casing subdomain is meshed with 7345 P1/P1 elements. Fig. 5(top) and (bottom) (left) show a zoom of the composite mesh near the casing corner at some time steps. In addition to the SGS stabilization technique, an anisotropic discontinuity capturing technique is used. The method is described in [3].

The time integration is carried out by the backward Euler scheme, with a time step of 2.32×10^{-4} s so that we impose approximately 10 times steps between two blade passings. We set both the relaxation parameters of the Dirichlet and Neumann conditions to 0.3 and perform 20 iterations per time step. As initial conditions, the inner subdomain is solved with zero traction and zero eddy viscosity flux. Then the outer subdomain is calculated by interpolating Dirichlet conditions from the solution on the inner subdomain. Note that for this example, the total time used by the master code is 3.7% of the total CPU time used to solve this problem. Fig. 4(top left) shows the good convergence of the problem.

Let us first check that the non-dimensional distance to the wall y^+ along the walls has reasonable values. Fig. 4(bottom left) and (bottom right) show the distribution of y^+ along one blade of the impeller and along the casing wall, obtained at time $t = 1.44 \times 10^{-2}$ s, once the periodic regime is achieved. We observe that as an average the computational wall falls within the turbulent zone of the boundary layer ($y^+ > 30$) and never reaches high values ($y^+ < 80$).

Fig. 4(top right) gives the variation of the pressure coefficient $c_p = 2p/\rho|\boldsymbol{U}|^2$ along the casing wall, at time $t = 1.44 \times 10^{-2}$ s. The starting point of the curve is the casing corner, while the upper left part of the curve is the outflow where the pressure is "weakly" zero. The figure shows the static pressure expansion undergone by the fluid as it flows along the casing wall to the outlet.

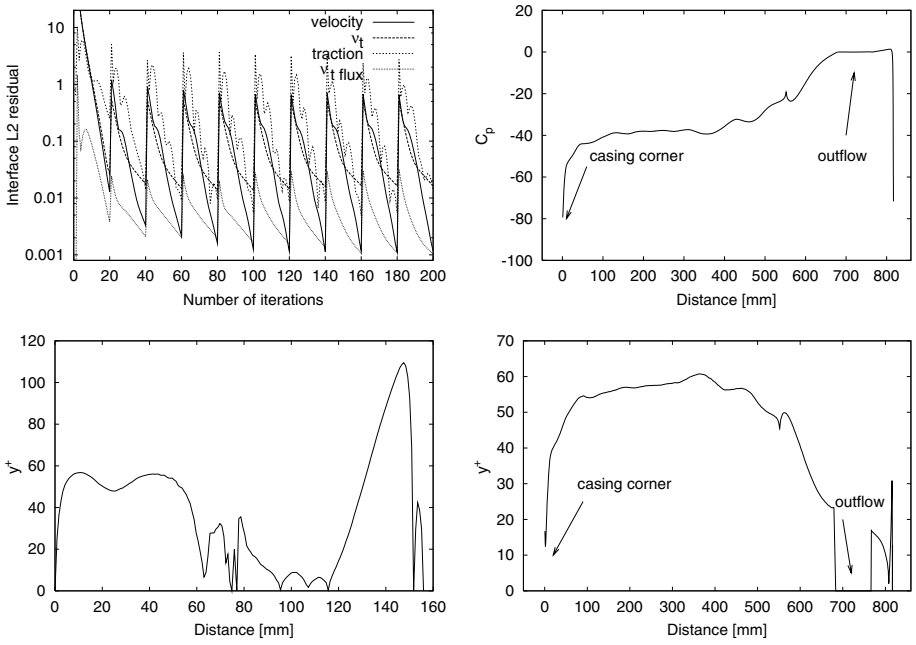

Fig. 4. CK-40 fan. (Top left) Convergence history. (Top right) Pressure along the casing wall. (Bottom left) y^+ along one blade. (Bottom right) y^+ along the casing wall.

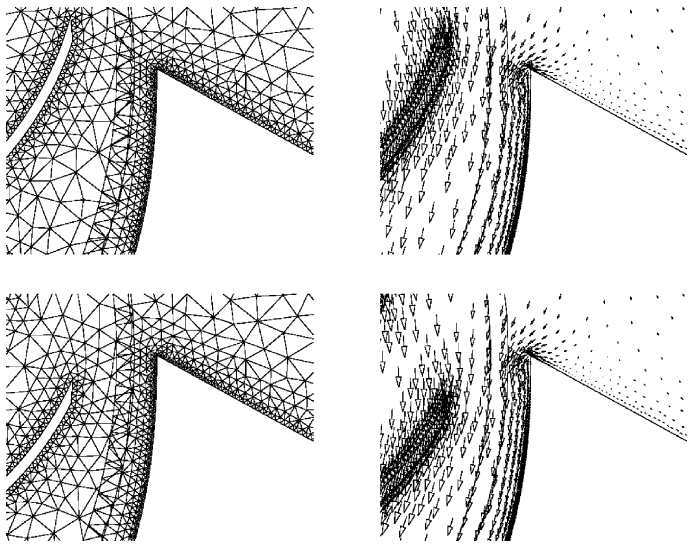

Fig. 5. CK-40 fan. (Left) Composite mesh. (Right) Velocity vectors near casing corner. (Top) $t = 5.75 \times 10^{-2}$ s. (Bottom) $t = 5.82 \times 10^{-2}$ s.

Fig. 5 aims at showing the incoming and outcoming character of the flow near the interface region. Fig. 6 shows the pressure and eddy viscosity contours.

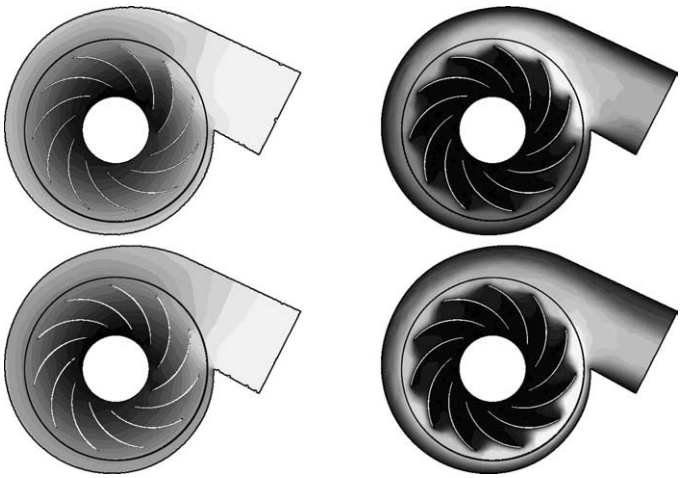

Fig. 6. CK-40 fan. (Left) Pressure contours. (Right) Eddy viscosity contours. (Top) $t = 5.75 \times 10^{-2}$ s. (Bottom) $t = 5.82 \times 10^{-2}$ s.

6. Conclusions

In this paper we have extended the overlapping Dirichlet/Neumann DD method proposed in a previous work to turbulent incompressible flows. With respect to disjoint methods, overlapping methods allow simpler divisions in subdomains, which is the case for example of the Chimera method. In addition, the proposed method has proved to be more robust than its disjoint counterpart. The method which uses here Dirichlet and Neumann transmission conditions can be extended straightforwardly to other mixed methods such as the Dirichlet/Robin method which exhibits better convergence properties [7,8]. In particular, in the case of disjoint subdomains, the convergence of the D/N method does depend on which interface we impose the Dirichlet condition while the D/R method inhibits this dependence.

References

[1] Codina R, Soto O. Finite element implementation of two-equation and algebraic stress turbulence models for steady incompressible flows. Int J Num Meth Fluids 1999;30:309–33.
[2] Bradshaw PB, Huang PG. The law of the wall in turbulent flows. Proc Roy Soc Lond A 1995;451:165–88.
[3] Codina R. A discontinuity-capturing crosswind-dissipation for the finite element solution of the convection–diffusion equation. Comp Meth Appl Mech Eng 1993;110:325–42.
[4] Codina R. A stabilized finite element method for generalized stationary incompressible flows. Comp Meth Appl Mech Eng 2001;190:2681–706.
[5] Houzeaux G, Codina R. Transmission conditions with constraints in finite element domain decomposition method for flow problems. Commun Numer Meth Eng 2001;17:179–90.
[6] Houzeaux G, Codina R. A geometrical domain decomposition method in computational fluid dynamics. Monograph CIMNE No. 70, December 2002.
[7] Houzeaux G, Codina R. An iteration by subdomain overlapping Dirichlet/Robin domain decomposition method for advection–diffusion problems, J Comput Appl Math, in press.

[8] Houzeaux G, Codina R. A Chimera method based on a Dirichlet/Neumann (Robin) coupling for the Navier–Stokes equations. Comp Meth Appl Mech Eng 2003;192:3343–77.
[9] Hughes Jr T. Multiscale phenomena: Green's functions, the Dirichlet-to-Neumann formulation, subgrid scale models, bubbles and the origins of stabilized methods. Comp Meth Appl Mech Eng 1995;127:387–401.
[10] Lions P-L. On the Schwarz alternating method I. In: Glowinski R, Golub GH, Meurant GA, Périaux J, editors. First International Symposium on Domain Decomposition Methods for Partial Differential Equations. Philadelphia, USA: SIAM; 1988. p. 1–42.
[11] Lube G, Müller L, Müller H. A new non-overlapping domain decomposition method for stabilized finite element methods applied to the nonstationary Navier–Stokes equations. Numer Lin Alg Appl 2000;7:449–72.
[12] Quarteroni A, Valli A. Domain decomposition methods for partial differential equations. Oxford Science Publications; 1999.
[13] Spalart PR, Allmaras SR. A one-equation turbulence model for aerodynamic flows. AIAA Paper 92-0439, 1992.
[14] Wilcox DC. Turbulence modeling for CFD. DCW Industries, Inc.; 1993.